PHYSICAL REVIEW B **91**, 241110(R) (2015)

Kitaev magnetism in honeycomb $RuCl_3$ with intermediate spin-orbit coupling

Heung-Sik Kim,[1] Vijay Shankar V.,[1] Andrei Catuneanu,[1] and Hae-Young Kee[1,2,*]

[1]*Department of Physics and Center for Quantum Materials, University of Toronto, 60 St. George St., Toronto, Ontario, Canada M5S 1A7*

[2]*Canadian Institute for Advanced Research, Toronto, Ontario, Canada M5G 1Z8*

(Received 26 November 2014; revised manuscript received 12 May 2015; published 19 June 2015)

Intensive studies of the interplay between spin-orbit coupling (SOC) and electronic correlations in transition-metal compounds have recently been undertaken. In particular, $j_{\text{eff}} = 1/2$ bands on a honeycomb lattice provide a pathway to realize Kitaev's exactly solvable spin model. However, since current wisdom requires strong atomic SOC to make $j_{\text{eff}} = 1/2$ bands, studies have been limited to iridium oxides. Contrary to this expectation, we demonstrate how Kitaev interactions arise in $4d$-orbital honeycomb α-$RuCl_3$, despite having significantly weaker SOC than the iridium oxides, via assistance from electron correlations. A strong-coupling spin model for these correlation-assisted $j_{\text{eff}} = 1/2$ bands is derived, in which large antiferromagnetic Kitaev interactions emerge along with ferromagnetic Heisenberg interactions. Our analyses suggest that the ground state is a zigzag-ordered phase lying close to the antiferromagnetic Kitaev spin liquid. Experimental implications for angle-resolved photoemission spectroscopy, neutron scattering, and optical conductivities are discussed.

DOI: 10.1103/PhysRevB.91.241110 PACS number(s): 71.70.Ej, 75.10.Jm, 71.20.Be, 75.30.Et

Introduction. Elucidating the cornucopia of novel physical phenomena exhibited by transition-metal compounds with electrons occupying d orbitals has been a key focus of modern condensed matter physics. Relativistic effects such as spin-orbit coupling (SOC), which entangles the spin and orbital degrees of freedom, were largely ignored until recently when it was realized that these effects in cohort with electronic correlations could give rise to new ground states, including those with uncommon magnetic ordering [1–8].

In particular, these effects bring about anisotropic exchange interactions that have been suggested as a way to engineer the exactly solvable Kitaev spin model [9] in the honeycomb iridate Na_2IrO_3. These anisotropic interactions arise between two neighboring iridium (Ir) sites, each with a single $j_{\text{eff}} = 1/2$ state, through superexchange mediated by the p orbitals on the intervening oxygen atoms that make up the edge-sharing octahedra around each Ir atom [10,11]. This $j_{\text{eff}} = 1/2$ state, composed of an equal mixture of t_{2g} orbitals, manifests at large SOC $\lambda \mathbf{L} \cdot \mathbf{S}$, where λ denotes the coupling strength, and $\mathbf{S}$ and $\mathbf{L}$ are spin and orbital angular momentum operators of the t_{2g} orbitals, respectively.

SOC is a relativistic effect roughly proportional to Z^4, where Z is the atomic number, and hence studies so far have been limited to iridium ($Z = 77$) and other heavy elements. Na_2IrO_3 and Li_2IrO_3, while good candidates, suffer from trigonal lattice distortions and diminished two dimensionality (2D) due to the Na atoms sandwiched between the honeycomb layers. The correct low-energy description is also under debate: single SOC-induced $j_{\text{eff}} = 1/2$ state versus nonrelativistic molecular orbitals [12,13]. Thus, the search for more ideal 2D honeycomb materials described by a $j_{\text{eff}} = 1/2$ picture is important.

Recently, it was suggested that a ruthenium chloride α-$RuCl_3$ ($RuCl_3$) is a good candidate because of its more ideal 2D honeycomb structure [14]. Although $RuCl_3$ should be metallic given the partially filled bands from the five valence electrons in t_{2g} orbitals, an insulating behavior is observed [15,16], suggesting the possibility of a Mott insulating phase driven by electron correlations. A natural question follows about the role of SOC; naively one would expect that it would not play a major part as atomic SOC in Ru is $\lambda \sim 0.1$ eV [17], a fraction of that in Ir.

In this Rapid Communication, we demonstrate that Kitaev magnetism can indeed be achieved in $RuCl_3$ despite its smaller atomic SOC strength. We arrive at this conclusion by first studying the role of electronic correlations using *ab initio* electronic structure calculations. The results are summarized in the schematic density of states (DOS) depicted in Fig. 1. The t_{2g} bands without SOC are shown in Fig. 1(a). In the presence of SOC, the bands near the Fermi level are mixtures of $j_{\text{eff}} = 1/2$ and $3/2$ shown in Fig. 1(b). This mixing is quite a contrast to the band structure of iridates, where the $j_{\text{eff}} = 1/2$ and $3/2$ bands are well separated. Nevertheless, when the on-site Coulomb interaction U is introduced while fixing a paramagnetic state, the bands near the Fermi level take on a predominantly $j_{\text{eff}} = 1/2$ character and a band gap develops as shown in Fig. 1(c), suggesting a correlation-induced insulating phase. We further derive a spin Hamiltonian and determine spin exchange parameters in the strong SOC limit employing tight-binding parameters obtained by projecting the *ab initio* band structure. We find that zigzag (ZZ) magnetic order has the lowest energy, and its corresponding band structure is shown in Fig. 1(d). We also discuss experimental tools to test our theory.

Ab initio calculations. $RuCl_3$ has a layered honeycomb structure and a d^5 valence electron configuration for Ru^{3+}, similar to the Ir^{4+} ion in Na_2IrO_3. While Na_2IrO_3 suffers from considerable lattice distortions, $RuCl_3$ has nearly perfect local cubic symmetry. Since the honeycomb layers of $RuCl_3$ are weakly coupled, we study a single honeycomb layer which should capture the important physics. We used OpenMX [18], which employs the linear-combination-of-pseudo-atomic-orbitals method for the electronic structure calculations and confirmed our results with the Vienna *Ab initio* Simulation Package [19,20]. Further details about our calculations are in the Supplemental Material [21].

*hykee@physics.utoronto.ca

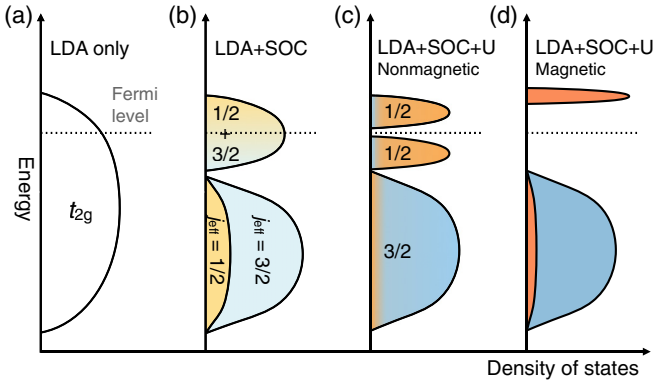

FIG. 1. (Color online) Schematic diagrams depicting the DOS and change in the electronic structure of $RuCl_3$ as SOC and the on-site Coulomb interactions are included. Red and blue colors represent the weights of $j_{\rm eff} = 1/2$ and $3/2$ states, respectively. Panel (a) displays the DOS without SOC, and panel (b) shows the DOS with SOC, which shows no clear separation between $j_{\rm eff} = 1/2$ and $3/2$ bands. On including U and fixing a paramagnetic state, as shown in panel (c), the bands near the Fermi level acquire $j_{\rm eff} = 1/2$ character and are separated from the $3/2$ bands. Panel (d) is the DOS in a magnetic ground state realized in $RuCl_3$.

The results of electronic structure calculations are presented in Fig. 2. Figure 2(a) shows the bands and projected density of states (PDOS) of $RuCl_3$ without SOC and electronic interactions. The long Ru-Cl and Ru-Ru bonds result in a Ru t_{2g} bandwidth of only 1 eV, significantly smaller than the bandwidth of honeycomb iridates [12,13,22,23]. The smaller bandwidth of $RuCl_3$ makes it more susceptible to SOC and correlations compared to its $5d$ counterparts. On the other hand, since each band in the t_{2g} manifold disperses across the entire bandwidth, the quasimolecular orbital picture suggested for Na_2IrO_3 is unsuitable for $RuCl_3$ [12]. Further clarification is provided in the Ssupplemental Material where the overlaps between the t_{2g} orbitals obtained by the maximally localized Wannier orbital method [24] is described.

In the presence of SOC, the band structure and PDOS projected onto the $j_{\rm eff}$ states are shown in Fig. 2(b). The magnitude of Ru SOC is found to be 0.14 eV, which is small compared to the bandwidth. While one can distinguish the $j_{\rm eff} = 1/2$ and $3/2$ bands near the Γ point, they are mixed with each other near the Brillouin zone boundaries, especially near the K point. PDOS shows that the $j_{\rm eff}$-projected weights of the $1/2$ and $3/2$ states near the Fermi level are comparable, showing that unlike its $5d$ counterpart Na_2IrO_3, SOC alone is insufficient to support the $j_{\rm eff} = 1/2$ picture in $RuCl_3$. The on-site Coulomb interactions in Ru d orbitals, however, does promote the $j_{\rm eff} = 1/2$ picture.

We performed LDA + SOC + U calculations fixing a paramagnetic (PM) phase to understand the combined effects of interactions and SOC without a magnetic order. Figure 2(c) shows the PM results with $U_{\rm eff} \equiv U - J_{\rm H} = 1.5$ eV ($J_{\rm H}$ is Hund's coupling), which is a metastable solution that can be obtained by slowly increasing $U_{\rm eff}$ from the noninteracting starting point. Compared to Fig. 2(b), one can see that the $j_{\rm eff} = 3/2$ states are pushed down significantly, so that the low-energy states near the Fermi level can be described purely in terms of the $j_{\rm eff} = 1/2$ states. The effective SOC at $U_{\rm eff} = 1.5$ eV is about twice the atomic value, a dramatic enhancement compared to results reported for iridates recently [25]. Previously, such an enhancement was reported for the $4d$ transition-metal oxide Sr_2RhO_4 [26].

Having established how correlations lead to a $j_{\rm eff} = 1/2$ picture in $RuCl_3$, we studied the energies of five different magnetic phases shown in Fig. 3(a): ferromagnet (FM), antiferromagnet (AF), stripy (ST), zigzag (ZZ), and 120 order. The relative energy differences between these phases as a function of $U_{\rm eff}$ is shown in Fig. 3(b). We find that the ZZ phase is the ground state over the entire range of $U_{\rm eff}$ up to 3.5 eV, except at $U_{\rm eff} = 1.0$ eV where the FM phase has lower energy. In the higher $U_{\rm eff}$ regime, ZZ is nearly degenerate with FM and 120 ordering. The electronic band structure for this ZZ state is shown in Fig. 2(d). After the magnetic order sets in, the $j_{\rm eff} = 1/2$ bands are further pushed away (the gap increases), and the occupied $j_{\rm eff} = 1/2$ band is now mixed with the $j_{\rm eff} = 3/2$ bands.

$j_{\rm eff} = 1/2$ spin model in the strong-coupling limit. As $RuCl_3$ is considered a Mott insulator [14], we construct a strong-coupling spin model to capture the possible magnetic phases of $RuCl_3$. Our analysis of correlation enhanced SOC allows us to construct a spin model based on pseudospin $j_{\rm eff} = 1/2$ states near the Fermi level. On each bond we fix a spin direction γ and label the bond $\alpha\beta(\gamma)$ as in Fig. 4(a), with α and β being the remaining two spin directions. The spin Hamiltonian relevant for $RuCl_3$, obtained from *ab initio*

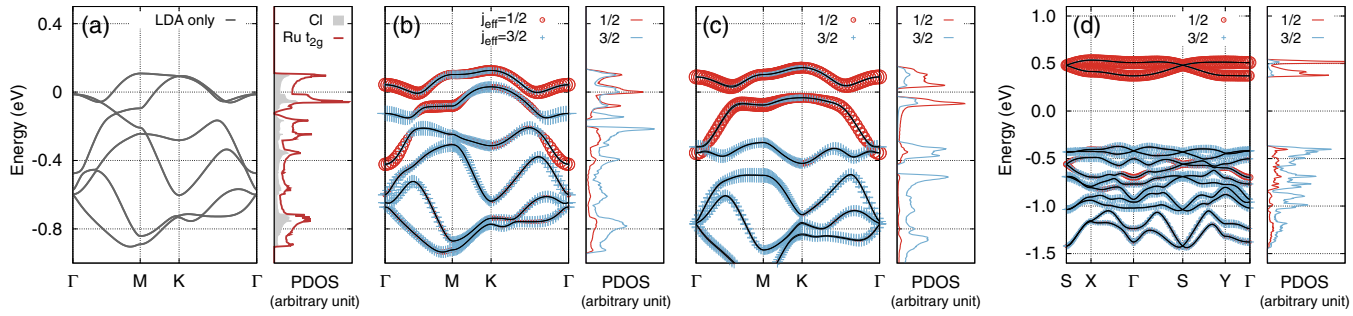

FIG. 2. (Color online) (a) Electronic structure of $RuCl_3$ without SOC and electron interactions. Red and gray curves depict the PDOS for Cl and Ru t_{2g}, respectively. The $j_{\rm eff}$-projected band structures and density of states are laid out in the presence of SOC in (b), SOC and the on-site Coulomb interaction of $U_{\rm eff} = 1.5$ eV while fixing a nonmagnetic state in (c), and with the lowest energy ZZ magnetic order in (d), respectively.

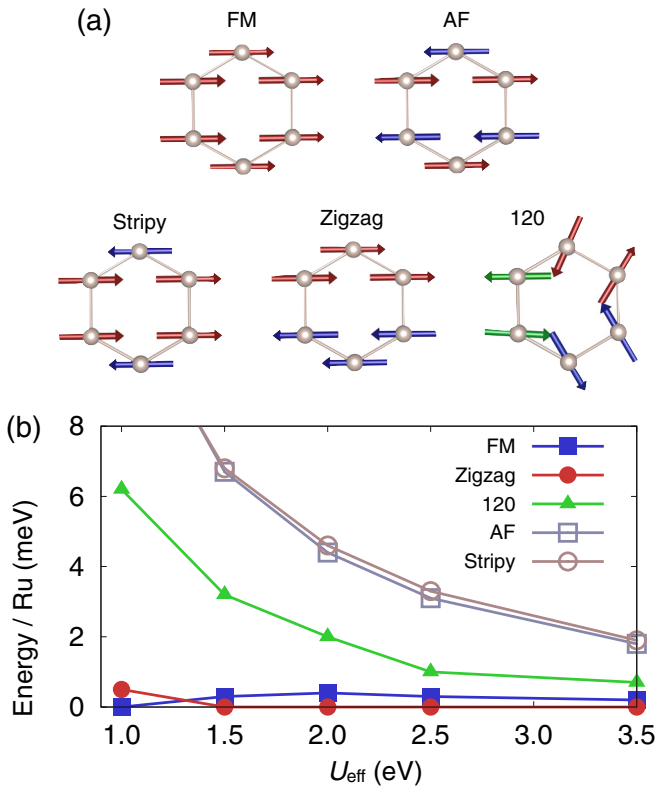

FIG. 3. (Color online) (a) Collinear magnetic configurations considered in the LDA+SOC+U calculations. (b) Relative energy difference per Ru atom for each configuration plotted with respect to $U_{\rm eff}$. The ZZ ordered state has the lowest energy except when $U_{\rm eff} = 1.0$ eV, but FM is competitive and the 120 ordered state approaches both states in energy when $U_{\rm eff}$ is large.

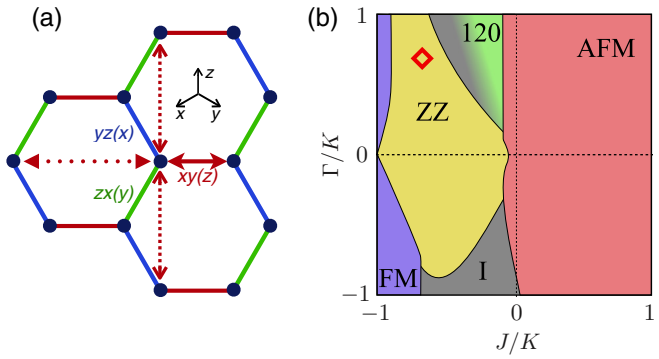

FIG. 4. (Color online) (a) First (solid), second (dashed), and third (dotted) NN bonds on the honeycomb lattice with the bond labels. Red, blue, and green colors depict the $\alpha\beta(\gamma) = xy(z)$, $yz(x)$, and $zx(y)$ bonds, respectively, where α, β, and γ denote the spin components interacting on the specified bond. Further neighbor hoppings with only $xy(z)$ type are depicted in the figure. (b) shows the Luttinger-Tisza phase diagram at $J_{\rm H}/U = 0.2$ for fixed second and third NN exchanges. Gray shading within the 120 order phase depicts the trace of incommensurate (I) order occurring in that area. The red diamond marks the estimated parameters for $RuCl_3$. See the main text for a description of the exchange parameters.

results is then

$$
\begin{aligned}
H = & \sum_{\langle ij\rangle\in\alpha\beta(\gamma)} \left[J\mathbf{S}_i\cdot\mathbf{S}_j + K S_i^\gamma S_j^\gamma + \Gamma\left(S_i^\alpha S_j^\beta + S_i^\beta S_j^\alpha\right)\right] \\
& + \sum_{\langle\langle ij\rangle\rangle\in\alpha\beta(\gamma)} \left(J_2^\alpha S_i^\alpha S_j^\alpha + J_2^\beta S_i^\beta S_j^\beta + J_2^\gamma S_i^\gamma S_j^\gamma\right) \\
& + \sum_{\langle\langle\langle ij\rangle\rangle\rangle\in\alpha\beta(\gamma)} \left[J_3\mathbf{S}_i\cdot\mathbf{S}_j + K_3 S_i^\gamma S_j^\gamma\right. \\
& \left. + \Gamma_3\left(S_i^\alpha S_j^\beta + S_i^\beta S_j^\alpha\right)\right], \qquad (1)
\end{aligned}
$$

where i,j label the Ru^{3+} sites and $\mathbf{S}_i$ is a $j_{\rm eff} = 1/2$ spin operator with components S_i^α. The parameters J and K are Heisenberg and Kitaev exchanges, respectively, and Γ is a symmetric off-diagonal exchange. $J_2^{(x,y,z)}$ are anisotropic spin exchanges at the second nearest-neighbor (NN) level, while J_3, K_3, and Γ_3 are the third NN analogs to the NN exchanges.

Since the exchanges are expressed in terms of overlaps between t_{2g} states, the on-site Coulomb interaction U, and the Hund's coupling $J_{\rm H}$, they can be estimated using the tight-binding parameters deduced from the *ab initio* calculations. For fixed $J_{\rm H}/U = 0.2$, we find that the NN terms dominate with antiferromagnetic K, ferromagnetic J, and positive Γ. Including NN t_{2g}-e_g exchange processes in addition to the ones within t_{2g}, we estimate the NN exchanges to be $J/K \simeq -0.7$ and $\Gamma/K \simeq 0.7$. The estimates for the second NN exchanges on a z bond denoted by red dashed lines in Fig. 4 are $J_2^x/K \simeq -0.03$, $J_2^y/K \simeq -0.01$, $J_2^z/K \simeq -0.01$ and those for third NN are $J_3/K \simeq 0.02$, $K_3/K \simeq 0.03$ with vanishingly small Γ_3/K. We note that the Kitaev exchange is further enhanced due to interorbital t_{2g}-e_g hopping [27]. For more details, including explicit expressions for the exchanges and tight-binding parameters, see the Supplemental Material.

Luttinger-Tisza analyses [28] were performed to obtain classical ground states of the above model. A phase diagram for varying J/K and Γ/K while keeping $J_2^{(x,y,z)}/K$, J_3/K, and K_3/K fixed is presented in Fig. 4(b). Based on the strength of the exchanges (see Supplemental Material) we find that the relevant position for $RuCl_3$, denoted by a red diamond in Fig. 4(b), is in the ZZ regime close to FM and 120 ordered states. While the qualitative features of the phase diagram are well captured by the NN J-K-Γ model, the addition of second and third NN exchanges enlarges the ZZ region. This enhancement of the ZZ phase on adding further neighbor exchanges was also observed for $J_H/U = 0.3$ and is likely independent of the J_H/U ratio. Our analysis predicts that $RuCl_3$ has a zigzag ordered ground state, described by a pseudospin $j_{\rm eff} = 1/2$ model, lying close to the antiferromagnetic Kitaev spin liquid. It is remarkable that the ZZ phase is surrounded by FM and 120 ordered phases in the strong-coupling phase diagram; these states are also found to be very close in energy in our LDA+SOC+U calculations.

Discussion and conclusion. There are various experimental ways to test our proposal. One experimental technique is angle-resolved photoemission spectroscopy, which is ideal for $RuCl_3$ with its layered structure. Occupied states below the Fermi level should reflect a large gap as well as flat dispersion across the Brillouin zone.

In the iridates, the first measurement that stimulated the idea of Sr_2IrO_4 being a spin-orbit Mott insulator was the optical conductivity, where an optical gap of around 0.5 eV was seen [29]. In $RuCl_3$ however, previous optical data was interpreted in terms of a small optical gap of 0.2–0.3 eV, but the extremely small intensity in this region suggests that this feature may not be associated with charge excitations [30]. Provided the optical gap is identified with the onset of the peak at around 1 eV in existing studies [14,15,31], which is bigger than the observed values of 0.5 eV in Sr_2IrO_4 [29] and 0.34 eV in Na_2IrO_3 [32], our results are in good agreement with the optical data.

Our prediction of ZZ magnetic order in the ground state, should be detectable by neutron scattering. An elastic neutron scattering measurement that has just been reported found a magnetic peak at the wave vector **M** below 8 K [33], suggesting that the magnetic order is either ZZ or ST. Based on the analysis of anisotropy in susceptibility provided in Refs. [33,34], we find an antiferromagnetic K, a ferromagnetic J which is a fraction of K, and a finite Γ. Thus, ZZ magnetic order should be consistent with both neutron and susceptibility data. Inelastic neutron scattering analysis, similar to the one reported for Na_2IrO_3 [35], can provide further confirmation, since the spin-wave spectra including spin gaps are different in the ZZ and ST phases. Thus computing spin-wave excitations in various regimes of the strong-coupling model would be a natural step for a future study.

It is important to note that although $RuCl_3$ shows a ZZ ordered phase similar to Na_2IrO_3, the microscopic origins of the two ZZ ordered phases are quite different. The Kitaev interaction is antiferromagnetic in $RuCl_3$,while it is ferromagnetic in Na_2IrO_3. This is because the Kitaev exchange originates from oxygen mediated hopping in Na_2IrO_3, while in $RuCl_3$, it is primarily due to direct overlap of d orbitals. The difference between the two compounds comes from the difference of covalency between oxygen and chlorine ions, suggesting that qualitative features of the underlying low-energy physics depends on structural and chemical details in these layered honeycomb compounds. The different magnetic ground states in Na_2IrO_3 and Li_2IrO_3 which shows an incommensurate spiral magnetic order [36] is another example. In this regard, a comparative study of $RuCl_3$ and Li_2RhO_3, which is isostructural and isoelectronic to Li_2IrO_3 [37], can be interesting as both share similar SOC strengths and electron correlations but have different lattice constants and p-orbital covalency.

In summary, combining *ab initio* and strong-coupling approaches, we have investigated the electronic and magnetic properties of $RuCl_3$. Our results strongly suggest that this compound can be understood as an interaction-driven $j_{\text{eff}} = 1/2$ system, which hosts magnetism dominated by the Kitaev interaction. Owing to the simple and ideal crystal structure, $RuCl_3$ provides an excellent platform to explore the physics of SOC and electronic correlations as well as related unconventional magnetism. Our study also opens up the possibility of a whole new class of materials in which to explore physics driven by spin-orbit coupling and electronic correlations, beyond the 5d transition-metal oxides.

Acknowledgments. We thank Y.-J. Kim, K. S. Burch, L. Sandilands, and E. K. H Lee for useful discussions and R. Schaffer for a critical reading of the manuscript. This work was supported by the NSERC of Canada and the Center for Quantum Materials at the University of Toronto. Computations were mainly performed on the GPC supercomputer at the SciNet HPC Consortium. SciNet is funded by the Canada Foundation for Innovation under the auspices of Compute Canada; the Government of Ontario; Ontario Research Fund for Research Excellence; and the University of Toronto. H.S.K. thanks the IBS Center for Correlated Electron System at Seoul National University for additional computational resources and V.S.V thanks NSERC-CREATE for a graduate fellowship through the HEATER program.

[1] W. Witczak-Krempa, G. Chen, Y. B. Kim, and L. Balents, Annu. Rev. Condens. Matter Phys. **5**, 57 (2014).
[2] X. Wan, A. M. Turner, A. Vishwanath, and S. Y. Savrasov, Phys. Rev. B **83**, 205101 (2011).
[3] E.-G. Moon, C. Xu, Y. B. Kim, and L. Balents, Phys. Rev. Lett. **111**, 206401 (2013).
[4] J. Maciejko, V. Chua, and G. A. Fiete, Phys. Rev. Lett. **112**, 016404 (2014).
[5] D. Pesin and L. Balents, Nat. Phys. **6**, 376 (2010).
[6] M. J. Lawler, H.-Y. Kee, Y. B. Kim, and A. Vishwanath, Phys. Rev. Lett. **100**, 227201 (2008).
[7] Y. Chen and H.-Y. Kee, Phys. Rev. B **90**, 195145 (2014).
[8] Y. Chen, Y.-M. Lu, and H.-Y. Kee, Nat. Commun. **6**, 6593 (2015).
[9] A. Kitaev, Ann. Phys. (Amsterdam, Neth.) **321**, 2 (2006).
[10] G. Khaliullin, Prog. Theor. Phys. Suppl. **160**, 155 (2005).
[11] G. Jackeli and G. Khaliullin, Phys. Rev. Lett. **102**, 017205 (2009).
[12] I. I. Mazin, H. O. Jeschke, K. Foyevtsova, R. Valentí, and D. I. Khomskii, Phys. Rev. Lett. **109**, 197201 (2012).
[13] H.-S. Kim, C. H. Kim, H. Jeong, H. Jin, and J. Yu, Phys. Rev. B **87**, 165117 (2013).
[14] K. W. Plumb, J. P. Clancy, L. J. Sandilands, V. V. Shankar, Y. F. Hu, K. S. Burch, H.-Y. Kee, and Y.-J. Kim, Phys. Rev. B **90**, 041112(R) (2014).
[15] L. Binotto, I. Pollini, and G. Spinolo, Phys. Status Solidi B **44**, 245 (1971).
[16] I. Pollini, Phys. Rev. B **53**, 12769 (1996).
[17] W. W. Porterfield, *Inorganic Chemistry* (Academic, New York, 2013).
[18] T. Ozaki, Phys. Rev. B **67**, 155108 (2003); http://www.openmx-square.org.
[19] G. Kresse and J. Hafner, Phys. Rev. B **47**, 558 (1993).
[20] G. Kresse and J. Furthmüller, Phys. Rev. B **54**, 11169 (1996).
[21] See Supplemental Material at http://link.aps.org/supplemental/10.1103/PhysRevB.91.241110 for computational details and further information on tight-binding parameters and exchange interactions.
[22] K. Foyevtsova, H. O. Jeschke, I. I. Mazin, D. I. Khomskii, and R. Valentí, Phys. Rev. B **88**, 035107 (2013).

[23] C. H. Kim, H. S. Kim, H. Jeong, H. Jin, and J. Yu, Phys. Rev. Lett. **108**, 106401 (2012).
[24] N. Marzari and D. Vanderbilt, Phys. Rev. B **56**, 12847 (1997).
[25] H.-S. Kim, Y. Chen, and H.-Y. Kee, Phys. Rev. B **91**, 235103 (2015).
[26] G.-Q. Liu, V. N. Antonov, O. Jepsen, and O. K. Andersen, Phys. Rev. Lett. **101**, 026408 (2008).
[27] J. Chaloupka, G. Jackeli, and G. Khaliullin, Phys. Rev. Lett. **110**, 097204 (2013).
[28] J. M. Luttinger and L. Tisza, Phys. Rev. **70**, 954 (1946).
[29] B. Kim, H. Jin, S. Moon, J.-Y. Kim, B.-G. Park, C. Leem, J. Yu, T. Noh, C. Kim, S.-J. Oh *et al.*, Phys. Rev. Lett. **101**, 076402 (2008).
[30] L. J. Sandilands, Y. Tian, A. A. Reijnders, H.-S. Kim, K. W. Plumb, H.-Y. Kee, Y.-J. Kim, and K. S. Burch, arXiv:1503.07593.
[31] G. Guizzetti, E. Reguzzoni, and I. Pollini, Phys. Lett. A **70**, 34 (1979).
[32] R. Comin, G. Levy, B. Ludbrook, Z.-H. Zhu, C. Veenstra, J. A. Rosen, Y. Singh, P. Gegenwart, D. Stricker, J. N. Hancock, D. van der Marel, I. S. Elfimov, and A. Damascelli, Phys. Rev. Lett. **109**, 266406 (2012).
[33] J. A. Sears, M. Songvilay, K. W. Plumb, J. P. Clancy, and Y.-J. Kim, Phys. Rev. B **91**, 144420 (2015).
[34] J. G. Rau, Erik Kin-Ho Lee, and H.-Y. Kee, Phys. Rev. Lett. **112**, 077204 (2014).
[35] S. K. Choi, R. Coldea, A. N. Kolmogorov, T. Lancaster, I. I. Mazin, S. J. Blundell, P. G. Radaelli, Y. Singh, P. Gegenwart, K. R. Choi, S.-W. Cheong, P. J. Baker, C. Stock, and J. Taylor, Phys. Rev. Lett. **108**, 127204 (2012).
[36] Y. Singh, S. Manni, J. Reuther, T. Berlijn, R. Thomale, W. Ku, S. Trebst, and P. Gegenwart, Phys. Rev. Lett. **108**, 127203 (2012).
[37] I. I. Mazin, S. Manni, K. Foyevtsova, H. O. Jeschke, P. Gegenwart, and R. Valentí, Phys. Rev. B **88**, 035115 (2013).